NASA/TM-2002-211770

Compression Buckling Behavior of Large-Scale Friction Stir Welded and Riveted 2090-T83 Al-Li Alloy Skin-Stiffener Panels

Eric K. Hoffman, Robert A. Hafley, John A. Wagner, and Dawn C. Jegley
Langley Research Center, Hampton, Virginia

Robert W. Pecquet and Celia M. Blum
Lockheed-Martin Space Systems, New Orleans, Louisiana

William J. Arbegast
South Dakota School of Mines and Technology, Rapid City, South Dakota

August 2002

The NASA STI Program Office . . . in Profile

Since its founding, NASA has been dedicated to the advancement of aeronautics and space science. The NASA Scientific and Technical Information (STI) Program Office plays a key part in helping NASA maintain this important role.

The NASA STI Program Office is operated by Langley Research Center, the lead center for NASA's scientific and technical information. The NASA STI Program Office provides access to the NASA STI Database, the largest collection of aeronautical and space science STI in the world. The Program Office is also NASA's institutional mechanism for disseminating the results of its research and development activities. These results are published by NASA in the NASA STI Report Series, which includes the following report types:

- TECHNICAL PUBLICATION. Reports of completed research or a major significant phase of research that present the results of NASA programs and include extensive data or theoretical analysis. Includes compilations of significant scientific and technical data and information deemed to be of continuing reference value. NASA counterpart of peer-reviewed formal professional papers, but having less stringent limitations on manuscript length and extent of graphic presentations.

- TECHNICAL MEMORANDUM. Scientific and technical findings that are preliminary or of specialized interest, e.g., quick release reports, working papers, and bibliographies that contain minimal annotation. Does not contain extensive analysis.

- CONTRACTOR REPORT. Scientific and technical findings by NASA-sponsored contractors and grantees.

- CONFERENCE PUBLICATION. Collected papers from scientific and technical conferences, symposia, seminars, or other meetings sponsored or co-sponsored by NASA.

- SPECIAL PUBLICATION. Scientific, technical, or historical information from NASA programs, projects, and missions, often concerned with subjects having substantial public interest.

- TECHNICAL TRANSLATION. English-language translations of foreign scientific and technical material pertinent to NASA's mission.

Specialized services that complement the STI Program Office's diverse offerings include creating custom thesauri, building customized databases, organizing and publishing research results ... even providing videos.

For more information about the NASA STI Program Office, see the following:

- Access the NASA STI Program Home Page at ***http://www.sti.nasa.gov***

- E-mail your question via the Internet to help@sti.nasa.gov

- Fax your question to the NASA STI Help Desk at (301) 621-0134

- Phone the NASA STI Help Desk at (301) 621-0390

- Write to:
  NASA STI Help Desk
  NASA Center for AeroSpace Information
  7121 Standard Drive
  Hanover, MD 21076-1320

NASA / TM-2002-211770

Compression Buckling Behavior of Large-Scale Friction Stir Welded and Riveted 2090-T83 Al-Li Alloy Skin-Stiffener Panels

Eric K. Hoffman, Robert A. Hafley, John A. Wagner, and Dawn C. Jegley
Langley Research Center, Hampton, Virginia

Robert W. Pecquet and Celia M. Blum
Lockheed-Martin Space Systems, New Orleans, Louisiana

William J. Arbegast
South Dakota School of Mines and Technology, Rapid City, South Dakota

National Aeronautics and
Space Administration

Langley Research Center
Hampton, Virginia 23681-2199

August 2002

Acknowledgments

This work was conducted under Space Act Agreement 446, funded by Lockheed-Martin Space Systems.

Available from:

NASA Center for AeroSpace Information (CASI)
7121 Standard Drive
Hanover, MD 21076-1320
(301) 621-0390

National Technical Information Service (NTIS)
5285 Port Royal Road
Springfield, VA 22161-2171
(703) 605-6000

CONTENTS

LIST OF FIGURES

LIST OF TABLES

Abstract

To evaluate the potential of friction stir welding (FSW) as a replacement for traditional rivet fastening for launch vehicle dry bay construction, a large-scale friction stir welded 2090-T83 aluminum-lithium (Al-Li) alloy skin-stiffener panel was designed and fabricated by Lockheed-Martin Space Systems Company – Michoud Operations (LMSS) as part of NASA Space Act Agreement (SAA) 446. The friction stir welded panel and a conventional riveted panel were tested to failure in compression at the NASA Langley Research Center (LaRC). The present paper describes the compression test results, stress analysis, and associated failure behavior of these panels. The test results provide useful data to support future optimization of FSW processes and structural design configurations for launch vehicle dry bay structures.

Introduction

Friction Stir Welding (FSW) is a solid-state joining process developed by The Welding Institute (TWI) [Ref. 1]. Compared to traditional fusion welding techniques, FSW offers higher mechanical properties, simplified processing, fewer weld defects, and reduced weld distortion and residual stresses [Ref. 2-16]. FSW has been used to join aluminum alloys that previously were thought to be unweldable.

FSW is being investigated as a potential lower cost replacement for the riveted skin-stiffener panel construction of launch vehicle dry bay structures, such as the forward adapter, intertank, and aft skirt (Figure 1). A test program was established by Lockheed-Martin Space Systems Company – Michoud Operations (LMSS) to assess the performance of FSW skin-stiffener structure versus the equivalent riveted structure and to optimize the performance of skin-stiffener structure for the FSW process. The program included testing of coupons, sub-elements, and large-scale panels to establish design and fabrication parameters influencing performance. Initial coupon level testing of 2090-T83 Al-Li specimens to assess weld parameters demonstrated that the FSW lap shear joints had adequate shear strength in comparison to riveted lap shear joints [Ref. 17].

Initial sub-element testing, which compared the compression crippling strength of riveted and FSW single-stiffener specimens of 2090-T83 Al-Li, showed that the FSW specimen exhibited a higher initial buckling load, but lower crippling failure load than the riveted specimen [Ref. 17]. Compression buckling tests and analysis of large-scale 2090-T83 Al-Li multiple-stiffener panels fabricated by FSW and conventional riveting were conducted to complete the initial test program, and are reported herein. Fabrication and testing of the large-scale panels has provided data to support FSW process optimization for skin-stiffened launch vehicle dry bay structures.

Panel Description, Fabrication, and Inspection

Both the FSW and riveted panels were designed and fabricated at LMSS. The panels consisted of five roll-formed 0.052 in.-thick 2090-T83 Al-Li hat stiffeners and a 0.083 in.-thick 2090-T83 Al-Li face skin (Figures 2 and 3). Both panels measured 60 in. long by 33 in. wide. The hat stiffeners of the riveted panel were attached to the face skin using 3/16 - in. 2017-T4 aluminum rivets spaced 1.25 in. apart. The hat stiffeners of the FSW panel were attached to the face skins using a LMSS standard H13 steel FSW pin tool [Ref. 17]. The welds were performed on a vertical milling machine with simplified steel backing anvils and finger clamps (Figure 4a). The welding parameters used are proprietary to LMSS.

Following fabrication, the panels were non-destructively inspected using visual, ultrasonic, and radiographic techniques. With the exception of one cold lap defect (CLD), all welds passed both ultrasonic and radiographic inspection. The weldments exhibited the typical concentric ring pattern characteristic of the FSW process and no surface galling was observed (Figure 4b). It was noted, however, that excessive weld flash was present on the welds located in the central regions of the panel. The excessive weld flash suggests non-optimized weld parameters and/or insufficient clamping of the panel to the steel backing anvil. Visual inspection of the riveted and FSW panels also revealed bowing of

the stiffeners in the longitudinal direction and warping of the face skin in the transverse direction (Figure 3). The FSW panel showed significantly more distortion than the riveted panel, possibly due to the effects of the non-optimized FSW schedule employed and the simple anvil and clamping support system used.

During post-test examination, it was observed that two of the inner stiffeners on the riveted panel, and one of the outer stiffeners on the FSW panel, measured 0.044 in.-thick instead of the specified 0.052 in.-thick gage in the stiffener cap and web due to excessive localized chemical milling. The FSW weldment thickness was unaffected by the chemical milling; the flange thickness of all stiffeners was 0.052 in. nominal.

Experimental Procedures

Panel Preparation

Following inspection, the panels were shipped to NASA Langley Research Center (LaRC) for panel preparation, instrumentation, and testing. Because of the potential for column bending of the panels from load eccentricity induced by the longitudinal bowing and transverse warping, attempts were made to reduce the panel distortion. Both panels were first clamped to a flat surface, then a strongback, consisting of a 3/8 in.-thick aluminum plate, was bolted across the back surface of both panel ends as shown schematically in Figure 5. The panel ends and attached strongbacks were then potted together with Hysol TE-4351 aluminum-filled epoxy. Angle iron frames were constructed to contain the potted panel ends with attached strongbacks. The angle iron potting frames and strongbacks did not extend to the ends of the panel to ensure that loading was introduced into the panel and potting only. Following the potting operation, the potted specimen ends were machined flat and parallel to within 0.002 in.

Measurements of the panels were taken to determine the effectiveness of the strongbacks in flattening the panels. All measurements were conducted on a Brown and Sharpe 300 series automatic coordinate machine that uses a probe stylus for measurement. Relative height measurements were taken at fixed positions across the width of the panel corresponding to the bays between the stiffeners, stiffener caps, and edges at 1.0 - in. intervals along the length of the panel. After the incorporation of the strongbacks, the riveted and FSW panels still showed significant distortion along the panel length and width (Figure 6). Maximum out-of-plane distortion for the riveted panel was approximately 0.3 in. (Figure 6a) compared to 0.6 in. for the FSW panel (Figure 6b).

Instrumentation

Sixty strain gages were used to measure strain in each of the test panels. A schematic of the strain gage positions on the test panel is shown in Figure 7. Axial (longitudinal) strain gages were placed on the stiffened and unstiffened sides of the panel at the same relative axial positions. Strain gage rosettes were placed on the opposing sidewalls of each of the five hat stiffeners. Out-of-plane displacements were recorded at five locations on the test panels. Direct current displacement transducers (DCDTs) were placed at four positions on the stiffened skin, in the center of bays 1 and 2 at the panel centerline location and 1.5 in. below the centerline. A DCDT was also placed on the center of stiffener cap 1 at the panel centerline. Additional DCDTs measured panel end shortening.

Moiré interferometry was used to qualitatively assess out-of-plane displacement of the panel surface. The unstiffened surface of each panel was painted white and a frame containing a Moiré fringe grating was placed in front of the panel. Illumination was then used to project the grating image onto the painted panel surface.

Test Procedures

Compression buckling tests were conducted in a 1000 kip hydraulic test machine at a constant crosshead displacement rate of 0.050 in./min (Figure 8). Load, strain, stroke, and displacement data were recorded at

1-second intervals during the tests. Video and still cameras recorded the Moiré interferometry pattern during loading. A 5000 lb. load was applied to the panel and strain gage output at the top of the panel was monitored to ensure that the load was being introduced into the panel uniformly. Shims were used between the loading platen and the potted end of the panel to ensure that strain variation at the top of the panel was less than 10%.

Prior to testing to failure, each panel was initially loaded to 50,000 lbs. and then unloaded to verify the correct operation of the instrumentation and to determine that the load was being introduced into the structure uniformly. This pre-test left no permanent deformation in the panels as evidenced by the loading and unloading portions of the strain gage data. Each panel was then tested to failure.

Results and Discussion

Measured displacements, measured strains, Moiré interferometry patterns, failure mechanisms, and stress analysis are presented in this section for the riveted and FSW panels. Skin buckling occurred on both panels prior to panel failure. The riveted panel failed catastrophically and carried a maximum load of approximately 113,700 lbs. The FSW panel carried a maximum load of approximately 90,500 lbs. In contrast to the riveted panel, the FSW panel did not fail catastrophically, but instead continued to deform after the maximum load was reached until the test was terminated at 83,000 lbs.

End Shortening and Out-of-Plane Displacement

End shortening displacement results for the riveted and FSW panels are shown in Figure 9. The end shortening at maximum load was 0.184 in. and 0.141 in. for the riveted and FSW panels, respectively. The load-end shortening displacement relationship was linear in both panels for loads less than approximately 75,000 lbs. The slope of these curves and, therefore, the global stiffness of these panels was approximately equal. Both panels displayed nonlinear deformation behavior after the onset of permanent deformation at loads greater than 75,000 lbs. The nonlinear behavior differs between the two panels in that the FSW panel shows a lower local stiffness (i.e., carries less load) in this nonlinear range than the riveted panel.

Out-of-plane displacement results for the riveted and FSW panels are shown in Figures 10 and 11, respectively. The out-of-plane displacement was insignificant for loads less than 75,000 lbs. in either panel. However, the out-of-plane displacement measurements were restricted to bays 1 and 2 and stiffener 1 (Figure 7). Since the panels had initial geometric imperfections, all bays were not loaded uniformly.

Photographs of out-of-plane displacement patterns determined from Moiré interferometry are shown in Figures 12 and 13 for the riveted and FSW panels, respectively. In each panel, the displacement patterns in the unloaded condition (0 lbs.) show initial panel imperfections (Figures 12a and 13a). The Moiré patterns of the FSW panel at 46,000 lbs. shown in Figure 13b indicate that changes in the out-of-plane displacement have taken place. These changes indicate that buckles were forming in the skin in bay 4 while the remainder of the panel was not significantly deforming out-of-plane. No such behavior was observed in the riveted panel at 50,000 lbs. as shown in Figure 12b. By 80,000 lbs., buckles were evident in the FSW panel in bays 2, 3, and 4 (Figure 13d) while buckles were just beginning to form in the riveted panel in bays 2 and 4 (Figure 12c). In all cases, initial buckles were local to the skin between the stiffeners and formed as square half waves with a width and length equal to the stiffener pitch. Prior to failure, buckles formed in all skin bays and skin beneath the stiffeners in both panels (Figures 12d and 13e).

Strain

Strains measured at the centerlines of the bays and stiffeners for the riveted panel are shown in Figures 14 and 15, respectively. Similar data for the FSW panel are shown in Figures 16 and 17. Stiffener strains were measured on the top of the stiffener caps and on the unstiffened skin beneath the stiffeners. In each figure, solid lines represent strains on the stiffened side and dashed lines represent strains on the unstiffened side of the panel.

The riveted panel, which had fewer geometric imperfections, displayed more uniform strains across the panel. Strain results indicate that all bay skins between the stiffeners buckled at loads between 65,000 and 80,000 lbs. in the riveted panel (Figure 14). Only the centerline strain gages in bay 4 of the FSW panel indicated buckling at the lower load of approximately 60,000 lbs. (Figure 16). While the riveted panel failed catastrophically at the maximum load, some strains in the FSW panel show strain reversal after the maximum load was reached indicating that buckling was continuing after maximum loading.

The strains measured in the stiffener caps and the skin underneath the stiffeners show consistent linear behavior across the width of both panels for loads less than approximately 75,000 lbs. (Figures 15 and 17). In the riveted panel, for loads greater than 75,000 lbs., buckling of the skin did not significantly affect the strains in the stiffener caps. Strains in the skin under the riveted stiffeners increased rapidly, reaching a maximum of approximately 0.0045 in./in. at panel failure (Figure 15). In the FSW panel, for loads greater than 75,000 lbs., the skin buckling influenced the strain in stiffener caps 1, 2, and 4 with stiffener cap 1 showing the most significant effect (Figure 17). Nonlinear behavior was evident and included a decrease in the magnitude of the strain followed by an increase in strain. Strains in the skin under the stiffeners show reversal or rapid increases at loads greater than 85,000 lbs. As loading continued past the maximum value, strain in the skin under stiffener cap 3 even moved into the tensile regime.

Compression Buckling of the Skin

Once local skin buckling occurs, strain gradients become large and strain gage position is critical if measured strains are to be used to determine initial buckling. For both panels, the strain gages may not have been optimally positioned to measure the maximum strain or the most significant differences in back-to-back strain gages. In addition, since the stiffeners were effective in carrying load after the skin buckled, not enough change in slope was observed in the load-end shortening results to determine buckling load (Figure 9).

The DCDTs measured out-of-plane displacements in bays 1 and 2 and stiffener 1 only, so no information can be gained from them for the other two bays, which includes the bay that buckled first. For both panels, the best method to determine the onset of buckling was to examine the Moiré interferometry patterns for out-of-plane displacements. Photographic evidence indicated that the riveted panel skin began to buckle at a load of approximately 80,000 lbs. All bay skins of the riveted panel were buckled by 93,000 lbs. and the skin under each stiffener was also buckled prior to failure. In contrast, the FSW panel skin buckled in bay 4 at loads less the 50,000 lbs., and the skin in all bays was buckled by 80,000 lbs.

Panel Failure Mechanisms

Buckling initiated in the skin between the stiffeners in both panels prior to failure. Once skin buckling occurred, additional load was forced into the stiffeners, resulting in added stress in the stiffeners and in the joint between the skin and the stiffener flanges. The riveted panel failed catastrophically with damage occurring across the entire width of the panel at approximately the centerline location as shown in Figure 18a. The riveted panel exhibited several failure mechanisms including rivet pull-out through the stiffener flanges, flange tearing between the rivets, permanent buckling deformation between the rivets, and fracture across the stiffener caps (Figure 18b).

The FSW panel did not fail catastrophically, but continued to deform after maximum load was reached. The FSW panel exhibited no weld separation between the skin and stiffeners nor fracture of the skin or stiffeners. Permanent deformation remained in the FSW panel after load was removed. This permanent deformation, shown in Figure 19a, occurred across the entire width of the FSW panel at the panel centerline. Post-test examination of the welds indicated little, if any, damage, even at a location known to have a cold lap defect prior to testing (Figure 19b).

Performance of FSW vs. Riveted Skin-Stiffener Panels

In this initial test program, the FSW configuration was a direct substitution for riveted structure and, as such, was not optimized for the FSW process. The FSW skin-stiffener panel had a 20% lower panel failure load than the equivalent riveted panel. Prior skin-stiffener sub-element crippling tests showed a potential 8% to 11% reduction in crippling load for non-optimized FSW configurations as compared to riveted configurations [Ref. 17]. The significant distortion present in the large-scale FSW panel test article is a major contributor to the 20% reduction in panel failure load for the FSW panel as compared to the riveted panel. FSW skin-stiffener panel performance would be enhanced by processing and tooling refinements that reduce panel distortion and by optimizing the configuration for the FSW process.

Stress Analysis

A stress analysis conducted by LMSS predicted an initial skin buckling load of 98,500 lbs. for both panels and a panel failure load of 98,200 lbs. for the riveted panel and 95,500 lbs. for the FSW panel. The stress analysis was performed using the standard methods for plate buckling and crippling strength of composite shapes and sheet-stiffener panels in compression, provided in Section C7 of Bruhn [Ref. 18], and is typical for dry bay skin-stiffened panels. The analysis included initial plate buckling, section crippling, and column analysis. In addition, local stability of the hat stiffener section with effective skin was assessed using the finite strip method [Ref. 19] due to the relatively thin hat stiffener thickness (0.052 in.).

The skin buckling analysis assumed no panel imperfections and a long, flat, skin panel with simply supported edges. Due to design considerations and the anisotropic properties of 2090 Al-Li, the modulus of elasticity at 45 degrees to the rolling direction was used in the analysis. The panel failure analysis attempted to account for the out-of-plane bowing associated with initial panel distortion. Beam column effects from the bowed hat stiffeners were included in the panel failure analysis using Newark's methods [Ref. 20]. The analysis predicted a lower panel failure load for the FSW panel because it exhibited significantly greater distortion compared to the riveted panel. The panel analysis did not, however, account for the non-uniform load distribution that resulted from the initial panel distortion.

Both the riveted and FSW panels were analyzed using the same procedures except for assessing the stiffener-to-skin joint. The riveted panel was assessed and shown to be adequate for inter-rivet buckling, sheet wrinkling, and rivet tension [Ref. 18]. The FSW joint was assessed based on coupon level testing of 2090-T83 Al-Li specimens which demonstrated that the FSW lap joints had adequate strength [Ref. 17]. No special analysis techniques, or material properties, were used in the FSW analysis to account for the effects of the reduced yield strength associated with the dynamically recrystallized (DXZ) and heat affected zones (HAZ) of the friction stir weldment, or the possible presence of sheet thinning [Ref. 17]. The locally reduced weldment properties could impact the crippling allowable for the FSW panel and result in a lower compression capability. As a result, the FSW panel failure load would be expected to be less than the 95,500 lbs. predicted using standard methods for riveted panels.

Performance vs. Predictions

Table 1 compares predicted and actual skin buckling initiation loads for the riveted and FSW panels. Skin buckling initiated in different regions of the panel at different loads; therefore, a range of loads is given in

the table. Both the riveted and FSW panels experienced initial skin buckling well below the predicted values. Based upon Moiré interferometry, the skin buckling initiation load for the riveted panel was 10% to 19% lower than the predicted value while the skin buckling initiation load for the FSW panel was 19% to 54% lower.

Table 1. Comparison of Predicted and Actual Skin Buckling Initiation Loads for the Riveted and FSW Skin-Stiffener Panels.

Panel	Predicted Load, lbs.	Actual Load (as determined by strain gage data), lbs.	Actual Load (as determined by Moiré interferometry), lbs.
Riveted	98,500	65,000 – 80,000	80,000 – 89,000
FSW	98,500	60,000	46,000 – 80,000

Table 2 compares predicted and actual panel compression failure loads for the riveted and FSW panels. The panel failure load for the riveted panel was 15% higher than predicted while the panel failure load for the FSW panel was 5% lower than predicted.

Table 2. Comparison of Predicted and Actual Panel Failure Loads for the Riveted and FSW Skin-Stiffener Panels.

Panel	Predicted Load, lbs.	Actual Load, lbs.
Riveted	98,200	113,700
FSW	95,500	90,500

Several factors may have contributed to the differences between predicted and experimental values. The riveted and FSW panels were not within the normal tolerances typical for flight hardware. While the strongbacks and potting did reduce the distortion, both panels still exhibited longitudinal bowing and warping across the width. The fact that bay 4 of the FSW panel, in which skin buckling initiated at 46,000 lbs., is in the location of maximum panel distortion (Figures 3b and 6b), indicates the significance of the distortion on initial skin buckling and subsequent panel failure. The skin buckling analysis did not account for panel distortion; the panel failure analysis accounted for the bowed stiffeners, but did not fully account for the geometric imperfections or for the resulting non-uniform load distribution evident in the Moiré interferometry (Figures 12 and 13). The skin buckling and panel failure analyses did not include the effects of the global and local distortion of the skin or of the reduced thickness of selected stiffeners, which could have resulted in reduced load carrying capability. In spite of the initial geometric imperfections and reduced weldment properties, the FSW panel failure load was within 5% of prediction.

Concluding Remarks

This compression panel study was part of a program involving coupon, sub-element, and large-scale panel tests of FSW and equivalent riveted structural configurations. The purpose of the program was to assess the feasibility of using FSW to replace traditional rivet fastening for launch vehicle dry bay structure. In the present study, compression buckling tests and stress analyses were conducted on large-scale FSW and riveted 2090-T83 Al-Li skin-stiffener panels to evaluate their structural performance.

The FSW skin-stiffener panel had a 20% lower panel failure load than the equivalent riveted panel. The riveted panel failed catastrophically at maximum load; the FSW panel did not fail catastrophically, but continued to deform after maximum load. The failed riveted panel exhibited rivet pull-out, flange tearing, and stiffener fracture. The FSW panel sustained permanent deformation, however, no weld separation

between the skin and stiffeners was observed. Both the riveted and FSW panel experienced initial skin buckling at loads well below predicted values. Several factors contributed to the differences between the predicted and experimental values including distortion, geometric imperfections, and reduced weldment properties. Distortion played a significant role in the FSW panel performance. In spite of these factors, the riveted panel failed above analysis predictions and the FSW panel failure load was 5% less than the prediction.

In this initial test program, the tested FSW configuration was a direct substitution for the riveted structure and, as such, was not optimized for the FSW process. These compression panel test results and corresponding stress analyses provide a better understanding of the effects of the FSW process on skin-stiffener compression panel performance and provide data to support future FSW design and process optimization. FSW skin-stiffener panel performance would be enhanced by processing and tooling refinements that reduce panel distortion and by designs that seek to minimize the effects of the reduced strength of the weldment and to optimize the configuration for the FSW process.

References

1. W.M. Thomas. et al.:"Friction Stir Butt Welding", International Patent Appl. No. PCT/GB92/02203 and GB Patent Appl. No. 9125978.8, Dec. 1991, U.S. Patent No. 5,460,317.
2. Karl-Eric Knipstrom and B. Pekkari, Friction Stir Welding Process Goes Commercial, *Welding Journal*, vol. 76, Sept. 1997, pp. 55-57.
3. M. Ranes, A.O Kluken, and O.T. Midling, "Fatique Properties of As-welded AA6005 and AA6082 Aluminum Alloys in T1 and T5 Temper Condition", Trends in Welding Research, *Proceedings of the 4th International Conference*, June 5 - 8, 1995.
4. C.J. Dawes and W.M. Thomas,Friction Stir Process Welds Aluminum Alloys, *Welding Journal*, vol. 75, March 1996, pp. 41-45.
5. G. Liu, L.E. Murr, C.S. Niou, J.C. McClure and F.R Vega, Microstructural aspects of the friction stir welding of 6061-T6 aluminum, *Scripta Mater*., vol. 37, Aug. 1997, pp. 355-361.
6. C.G. Rhodes, M.W. Mahoney, W.H. Bingel, R.A. Spurling and C.C. Bampton, Effects of friction stir welding on microstructure of 7075 aluminum, *Scripta Mater*., vol. 36, Jan. 1997, pp. 69-75.
7. M.W. Mahoney, Properties of Friction-Stir-Welded 7075-T651 Aluminum, *Met Trans*, vol. 29A, no. 7, July 1998, pp. 1955-1964.
8. B.K. Christner and G.D. Sylva: "Friction Stir Weld Development for Aerospace Applications", *International Conference on Advances in Welding Technology*- Joining of High Performance Materials, Nov. 6-8 1996, Columbus, Ohio.
9. Z.S. Loftus, W.J. Arbegast, and P.J. Hartley: "Friction Stir Weld Tooling Development for Application on the 2195 Al-Li-Cu Space Transportation System External Tank", *Proceedings of the 5th International Conference on Trends in Welding Research*, Pine Mountain, GA, June 1-5, 1998.
10. W.J. Arbegast and P.J. Hartley: "Friction Stir Welding Technology Development at Lockheed Martin Michoud Space System – An Overview", *Proceedings of the 5th International Conference on Trends in Welding Research*, Pine Mountain, GA, June 1-5, 1998.
11. R. Braun, D.C. Dalle, and G Staniek: "Investigations of laser beam and friction stir welded Al joints", DLR Material Colloquium, December 11, 1997.
12. C.J. Dawes and W. Thomas: "Development of Improved Tool Designs for Friction Stir Welding of Aluminium", *1st International Symposium of Friction Stir Welding*, Los Angeles, CA, June 14-16, 1999.
13. D. Waldron: "Application of Friction Stir Welding for Delta Rocket Fuel Tanks", *1st International Symposium of Friction Stir Welding*, Los Angeles, CA, June 14-16, 1999.
14. W. Thomas: "Friction Stir Welding of Ferrous Materials; A Feasibility Study", *1st International Symposium of Friction Stir Welding*, Los Angeles, CA, June 14-16, 1999.

15. T.J. Lienert and J.E. Gould: "Friction Stir Welding of Mild Steel", *1st International Symposium of Friction Stir Welding*, Los Angeles, CA, June 14-16, 1999.
16. C.G. Anderson and R.E. Andrews: "Fabrication of Containment Canisters for Nuclear Waste by Friction Stir Welding", *1st International Symposium of Friction Stir Welding*, Los Angeles, CA, June 14-16, 1999.
17. B.J. Dracup and W.J. Arbegast, "Friction Stir Welding as a Rivet Replacement Technology", *Proceedings of the 1999 SAE Aerospace Automated Fastening Conference & Exposition*, Memphis, TN, October 5-7, 1999.
18. E.F. Bruhn, "Analysis and Design of Flight Vehicle Stuctures", S.R. Jacobs & Associates, Inc., 1973.
19. J.S. Przemienieki, "Finite Element Structural Analysis of Local Stability", AIAA Journal Volume 11, No. 1, January 1973.
20. N.M. Newmark, "Numerical Procedure for Computing Deflections, Moments, and Buckling Loads", pgs 1161-1234, ASCE Paper #2202, May 1942.

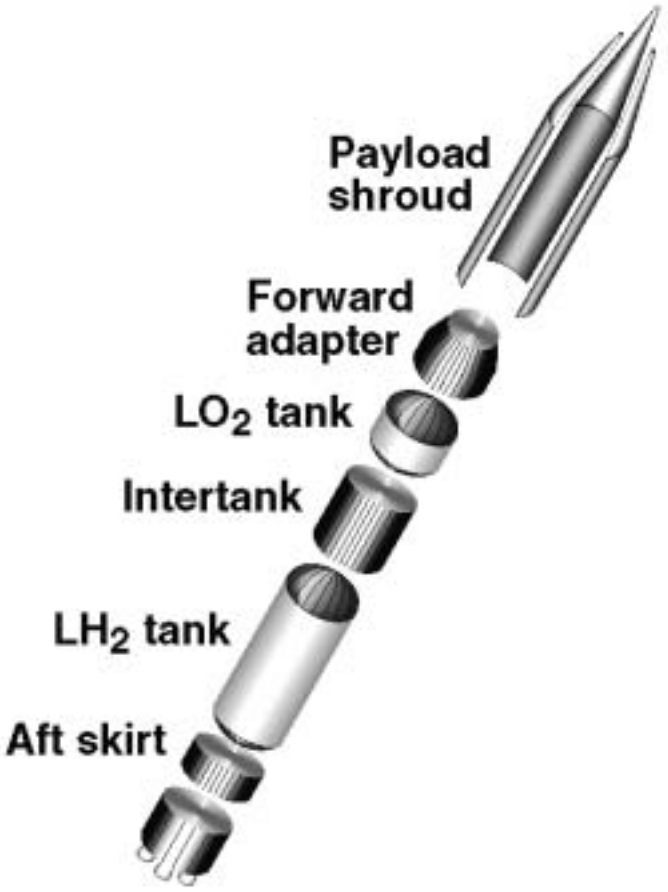

Figure 1. Typical launch vehicle configuration showing potential dry bay structure applications for friction stir welded skin-stiffener panels.

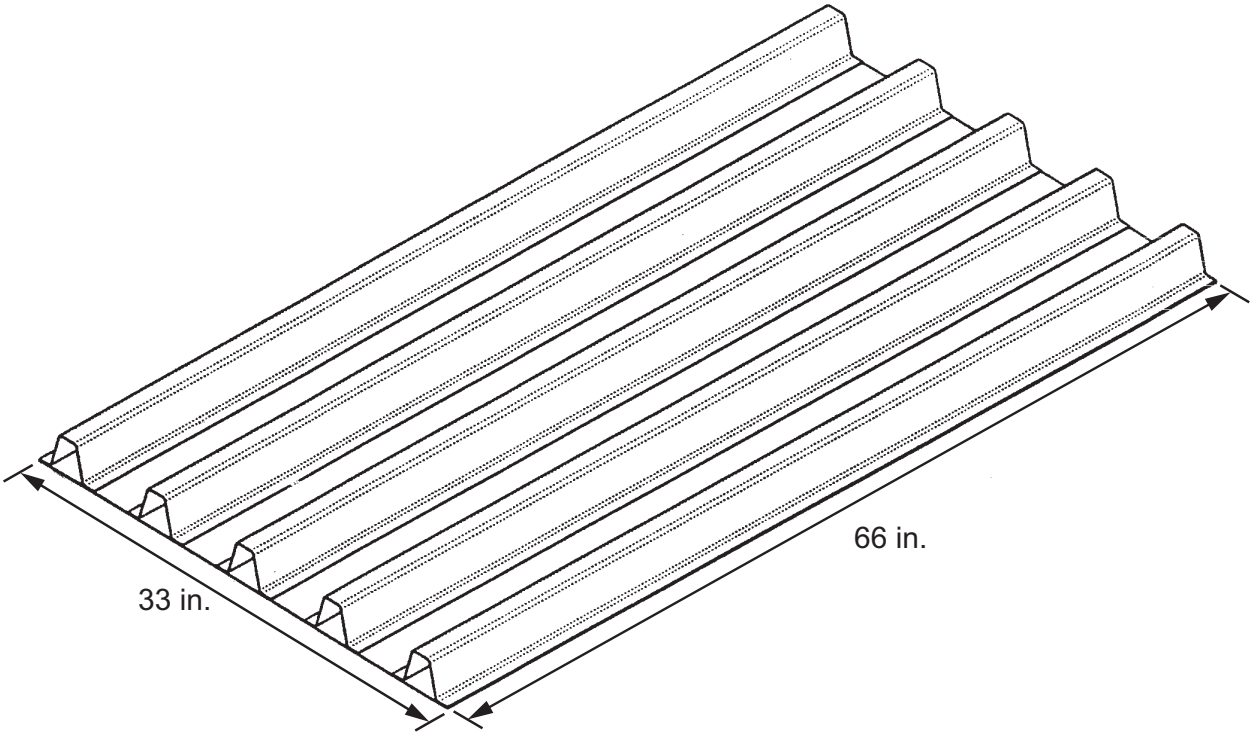

Figure 2. Schematic of skin-stiffener panel.

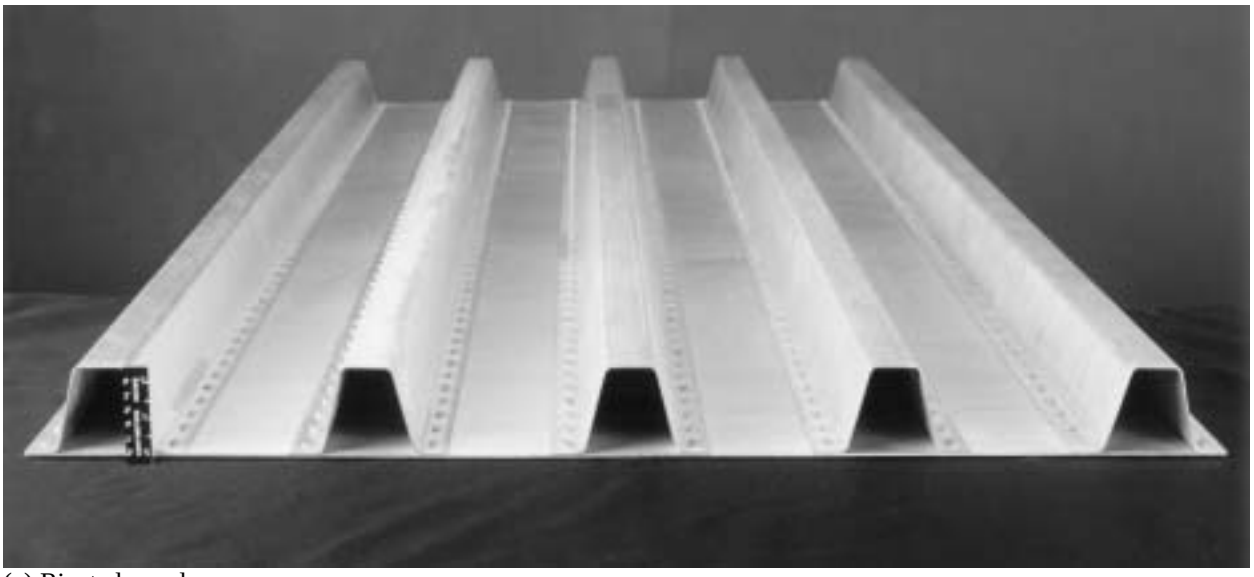

(a) Riveted panel.

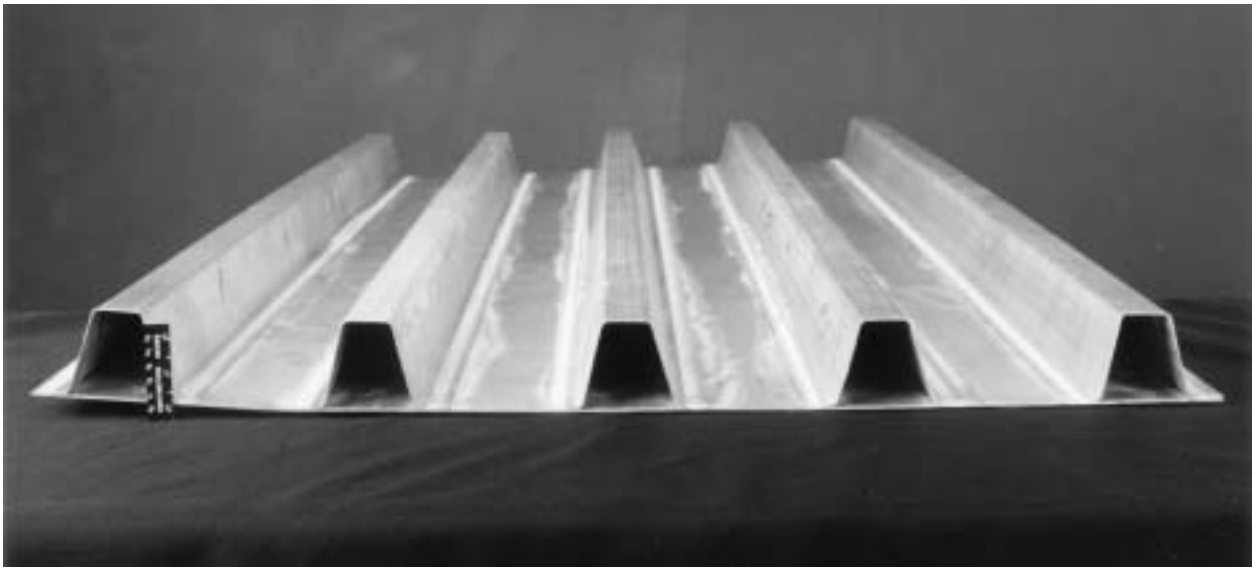

(b) Friction stir welded panel.

Figure 3. Photographs of riveted and friction stir welded skin-stiffener-test panels which exhibit panel warpage.

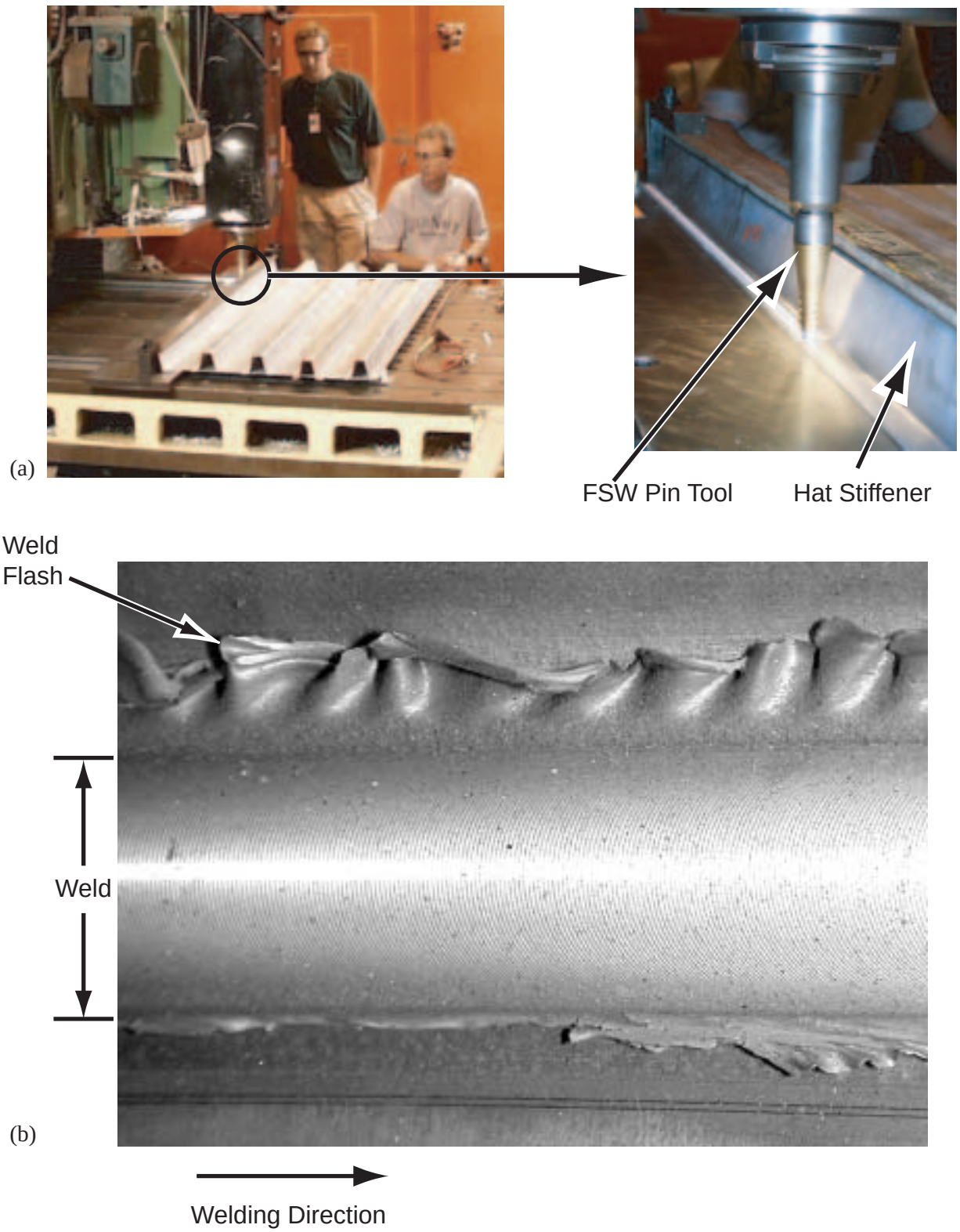

Figure 4. (a) FSW of skin-stiffener panel; (b) Friction stir weldment showing concentric ring pattern and weld flash.

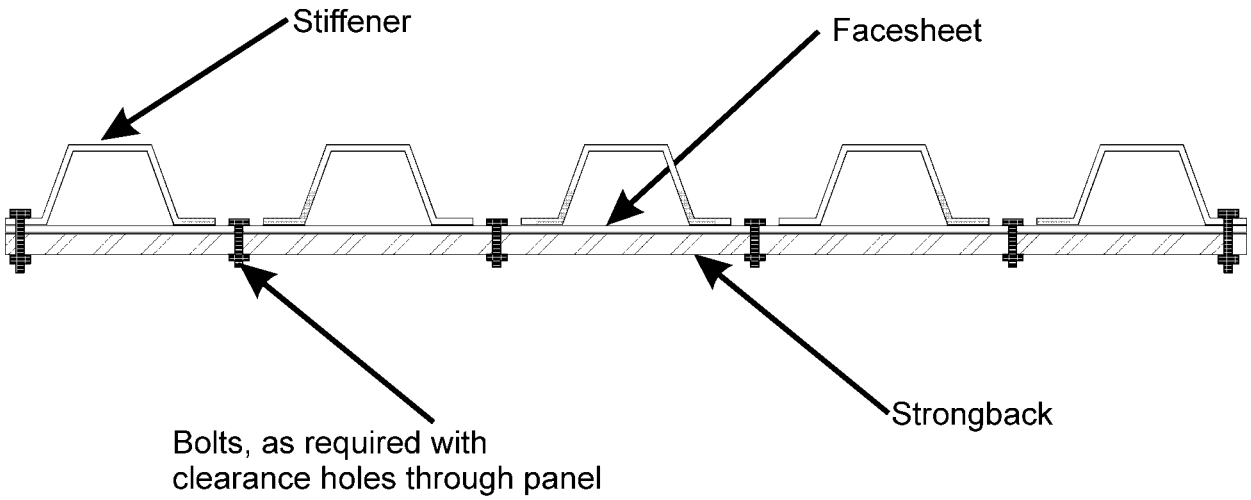

Figure 5. Schematic of strongback used to flatten panels.

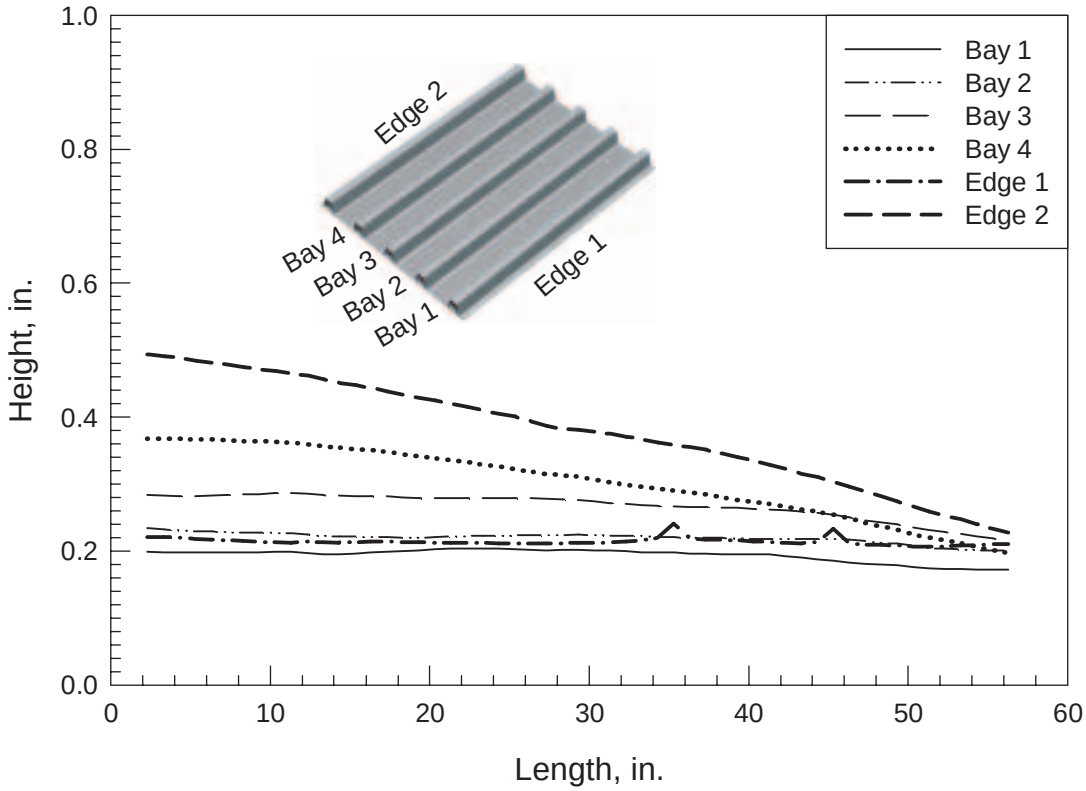

(a) Riveted panel.

Figure 6. Out-of-plane distortion of the riveted panel and the friction stir welded panel following strongback installation and potting.

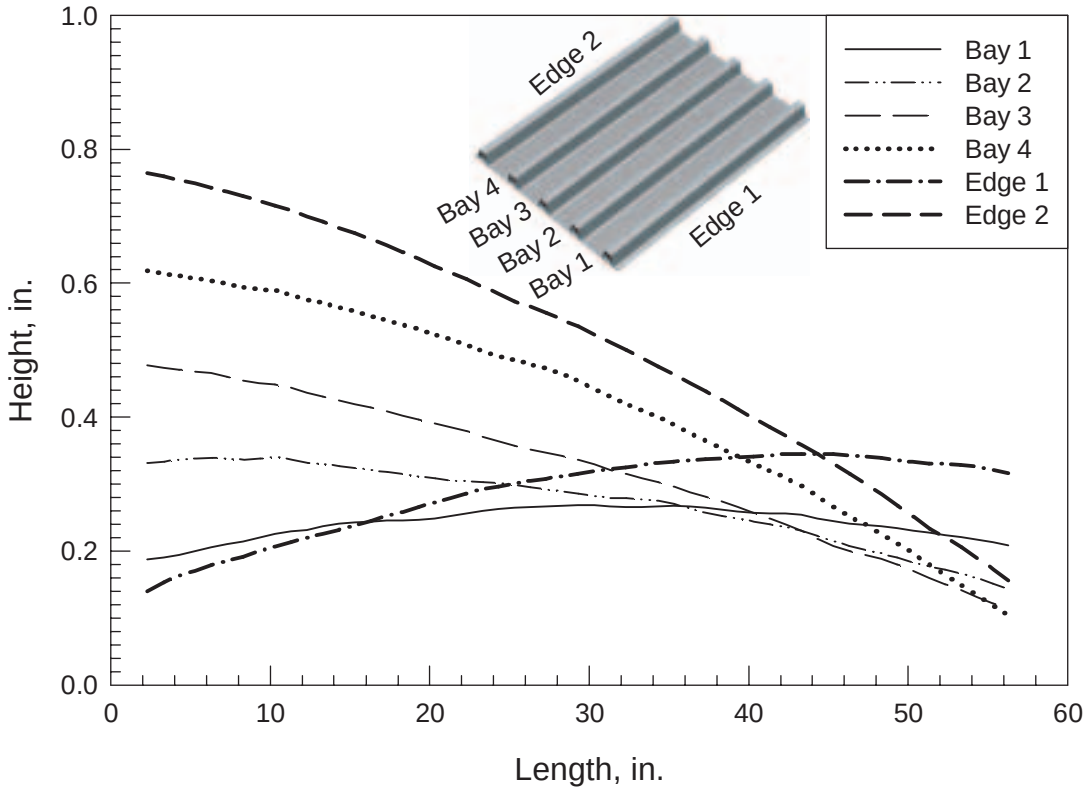

(b) Friction stir welded panel.

Figure 6. Concluded.

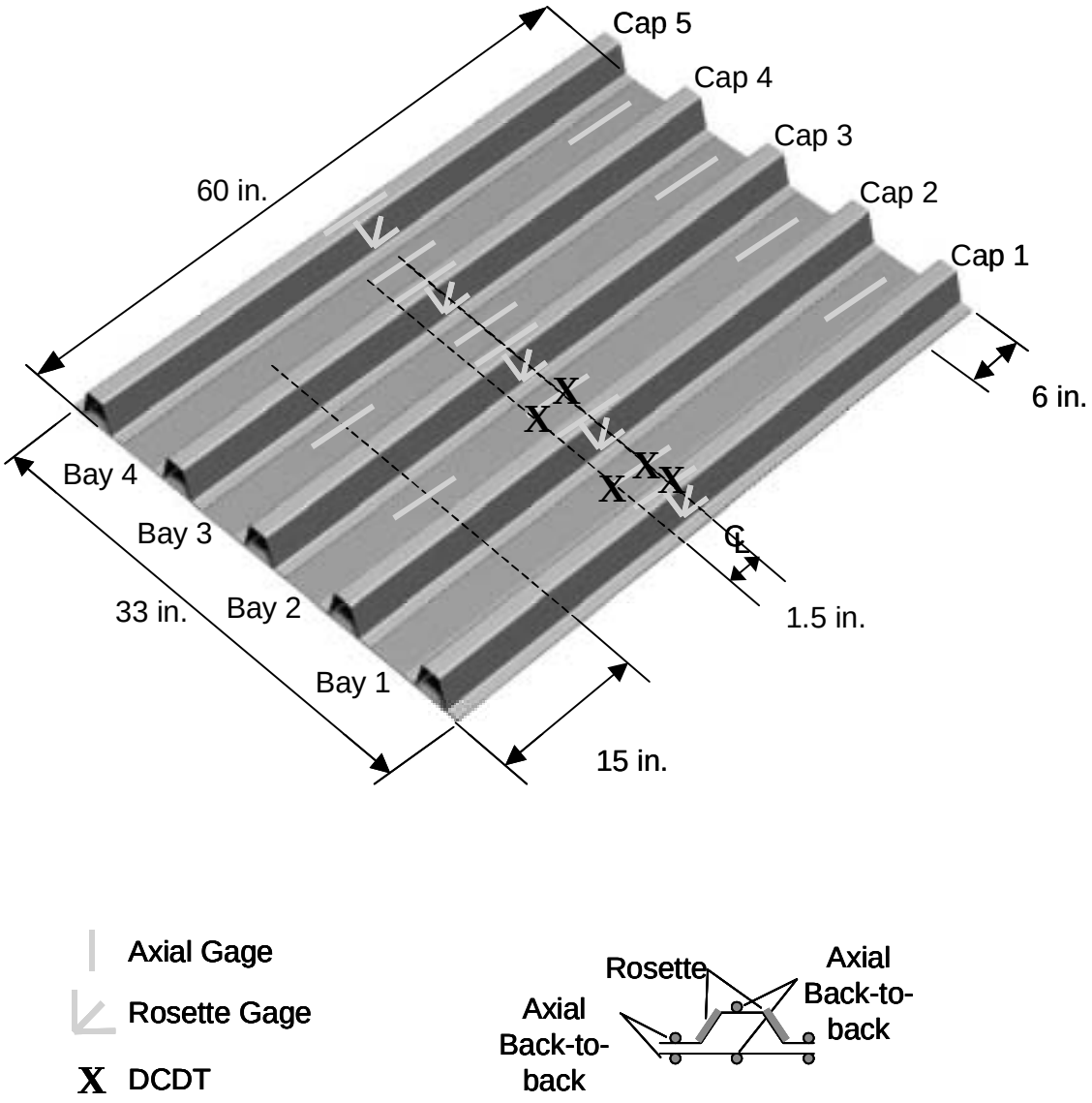

Figure 7. Schematic of test panel showing location of instrumentation.

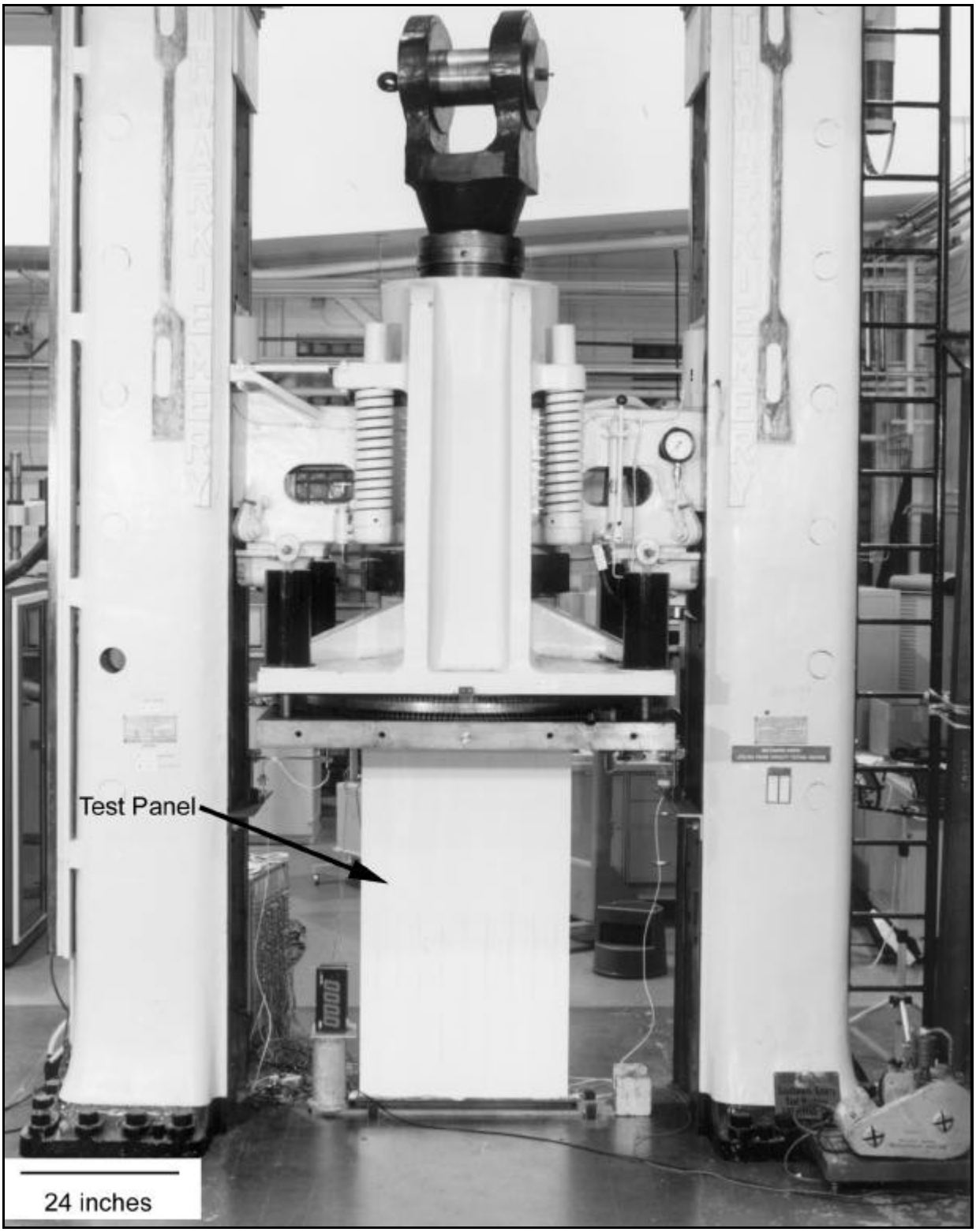

Figure 8. Test panel in the 1000-kip hydraulic test stand.

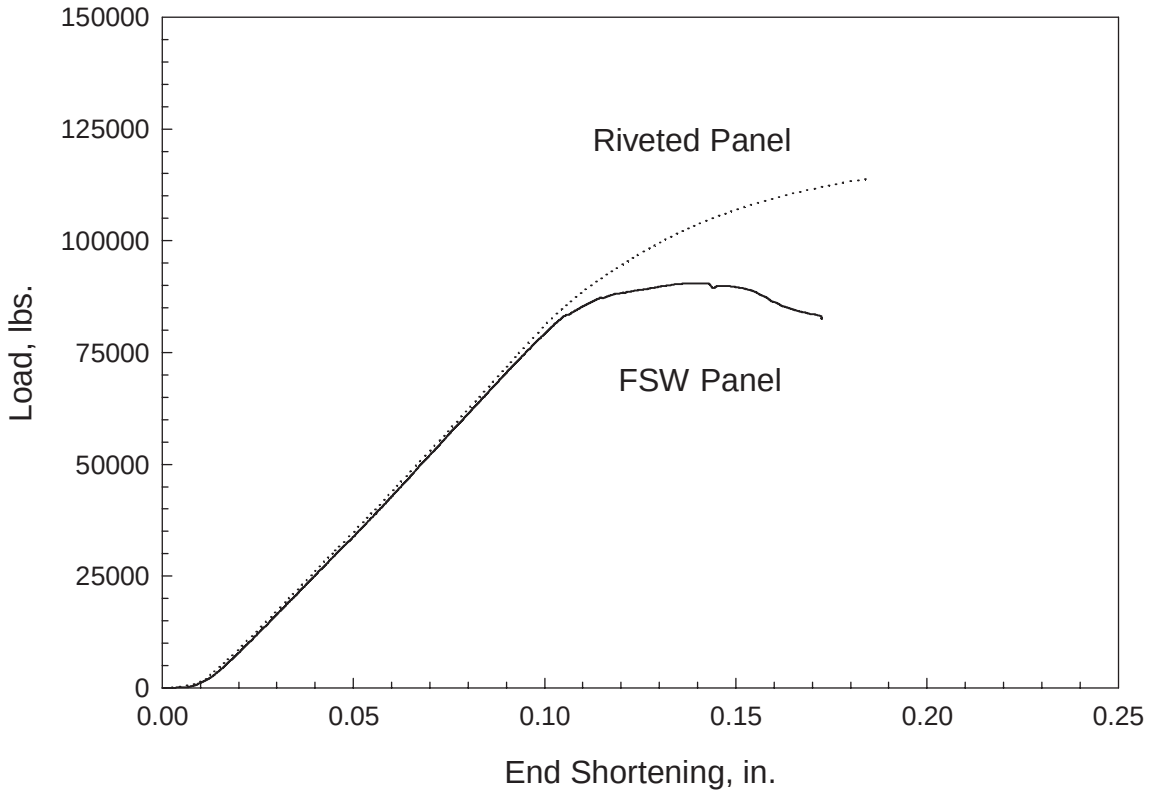

Figure 9. End shortening displacement of the riveted and friction stir welded panels.

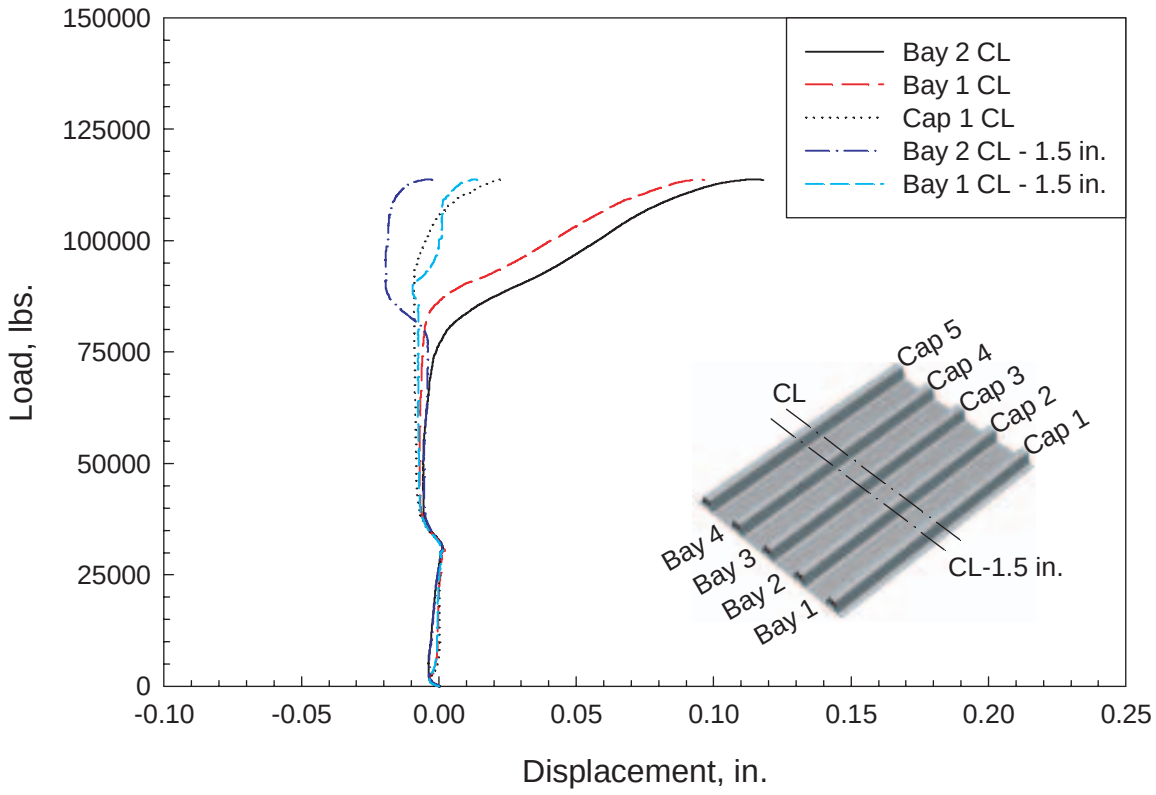

Figure 10. Out-of-plane displacement for the riveted panel.

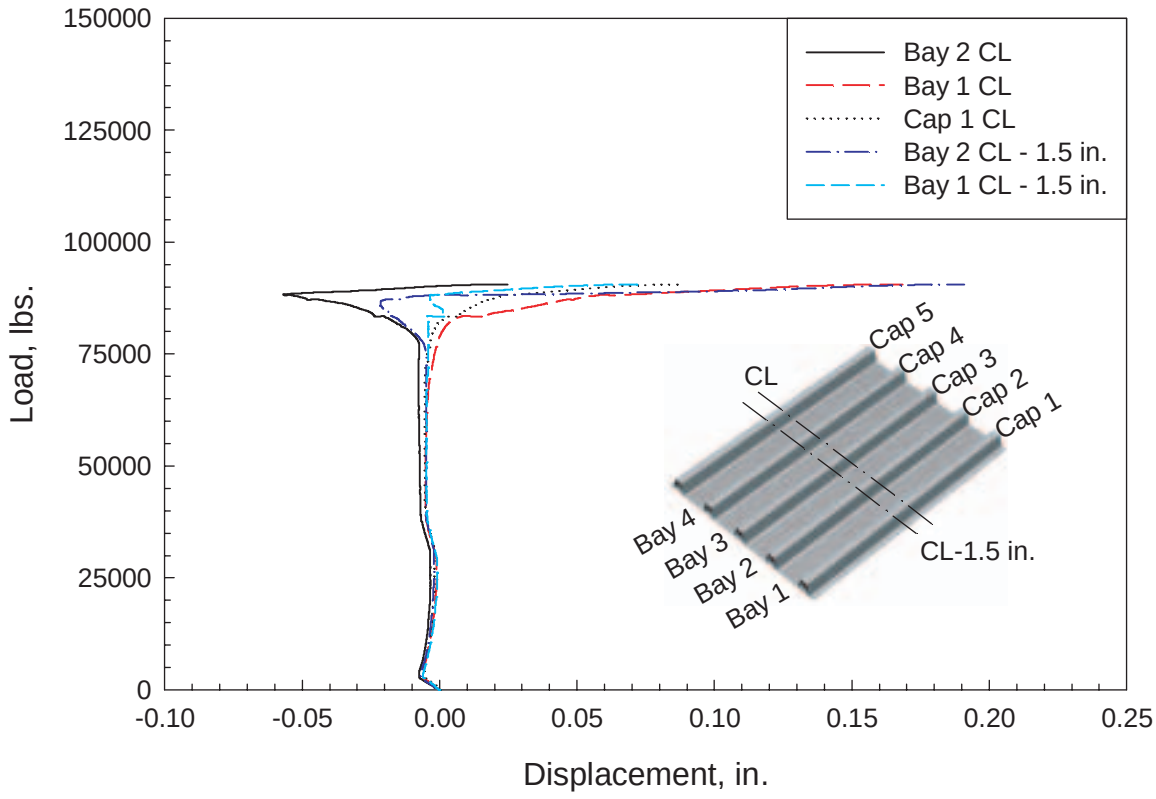

Figure 11. Out-of-plane displacement for the friction stir welded panel.

(a) 0 lbs.

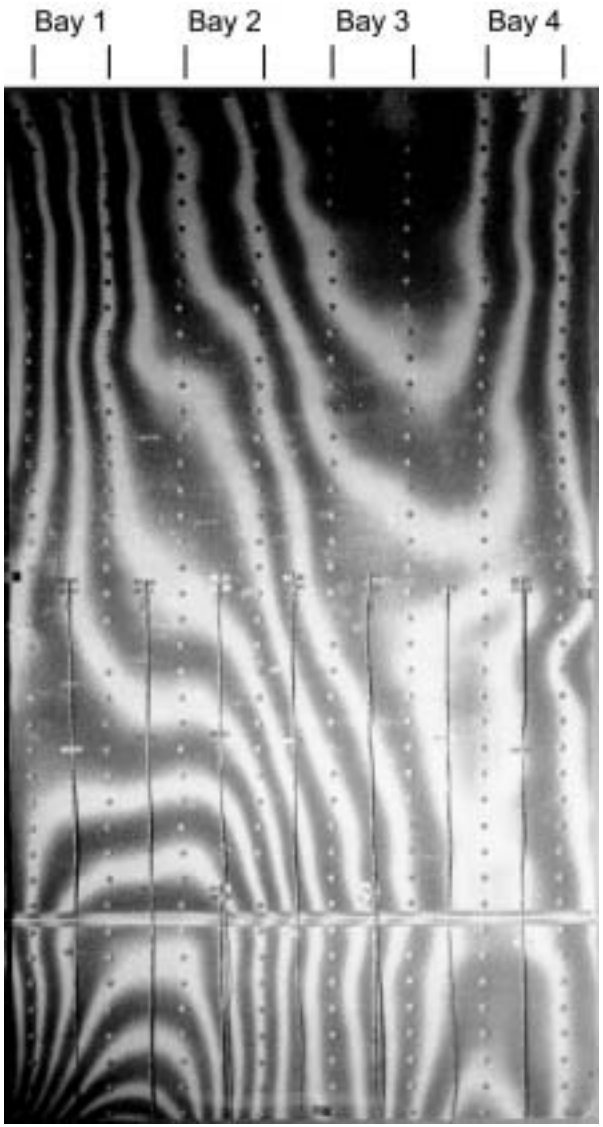

(b) 50,000 lbs.

Figure 12. Moiré interferometry patterns from the riveted panel at various load levels.

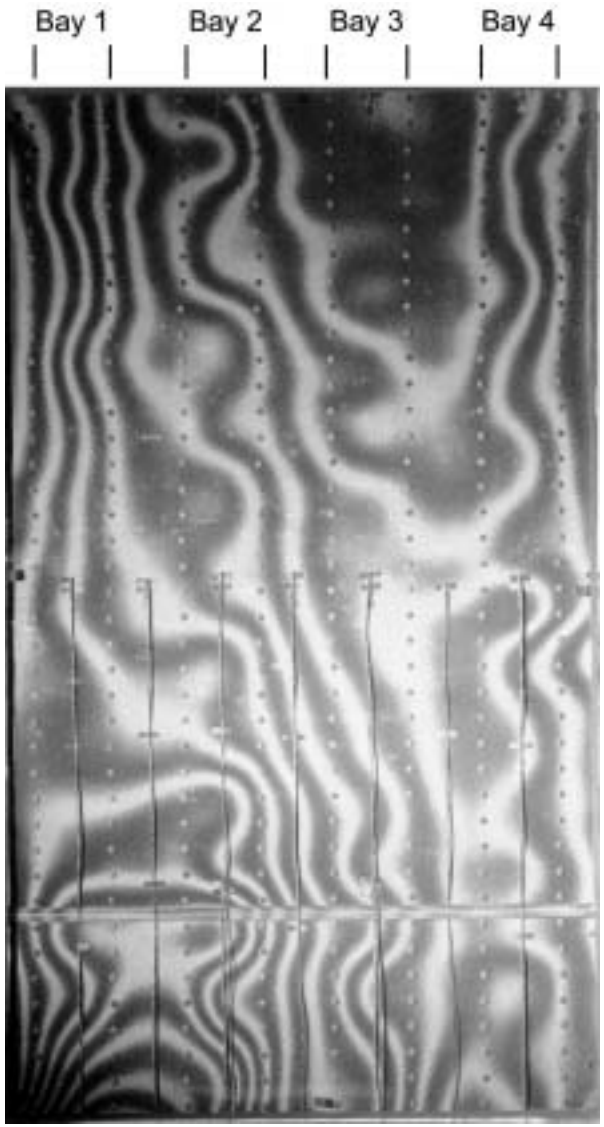

(c) 80,000 lbs.

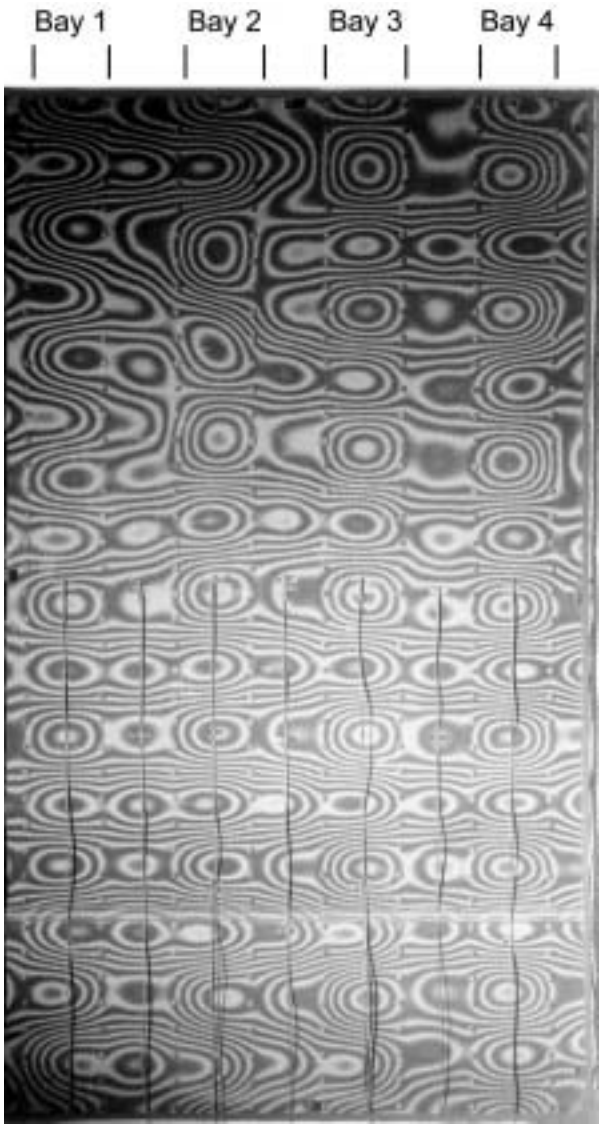

(d) 110,000 lbs.

Figure 12. Concluded.

(a) 0 lbs.

(b) 46,000 lbs.

Figure 13. Moiré interferometry patterns from friction stir welded panel at various load levels.

(c) 60,000 lbs.

(d) 80,000 lbs.

Figure 13. Continued.

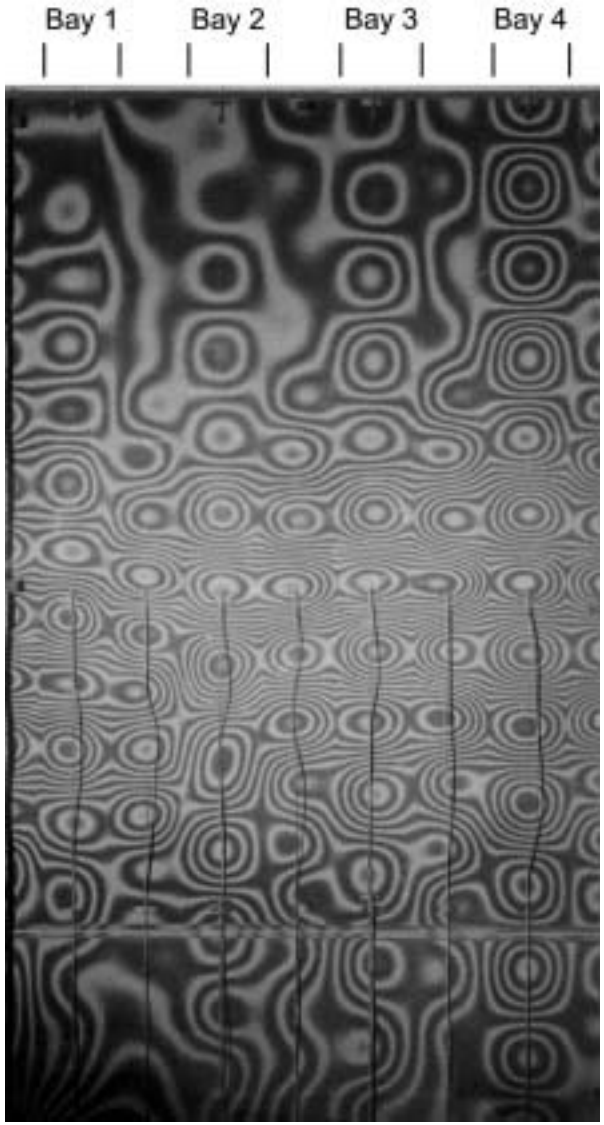

(e) 90,000 lbs.

Figure 13. Concluded.

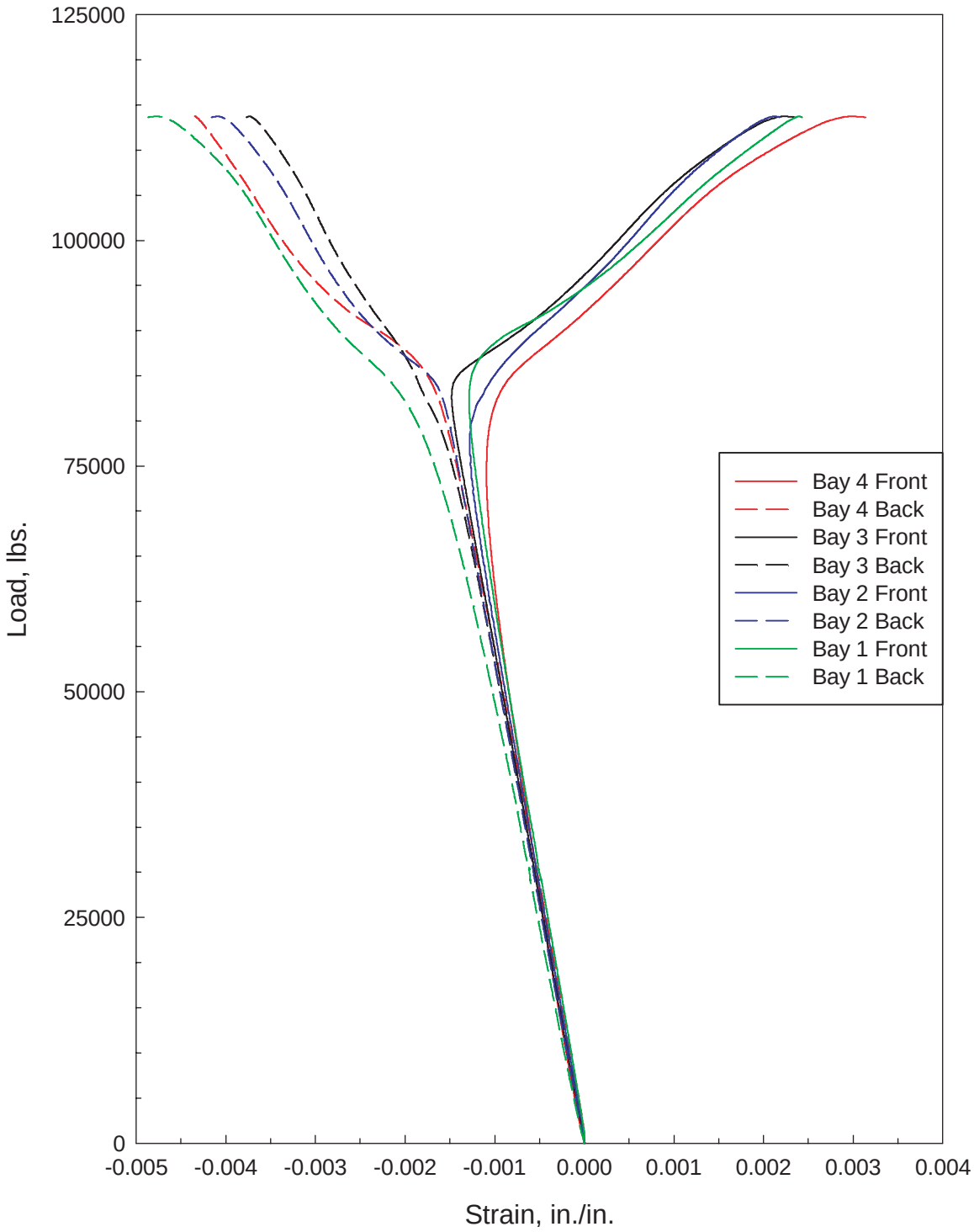

Figure 14. Strains at the centerline of the riveted panel bays. Solid lines represent the bay skin strains on the front, or stiffener, side of the panel and dashed lines represent the bay skin strains on the back, or unstiffened, side of the panel.

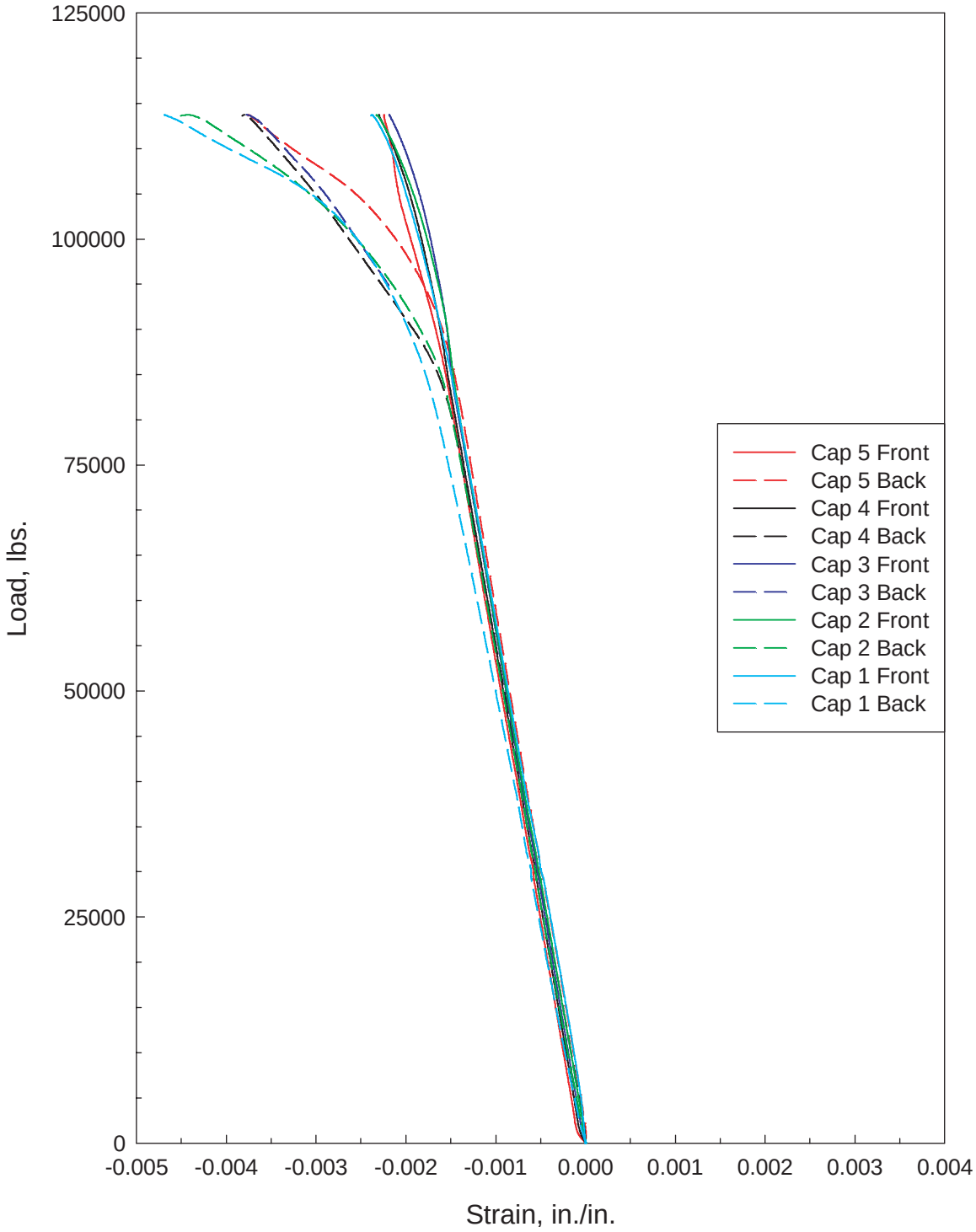

Figure 15. Strains at the centerline of the riveted panel stiffeners. Solid lines represent the strains on the top of the stiffener caps and the dashed line represent the strains on the skin beneath the stiffeners on the back, or unstiffened, surface.

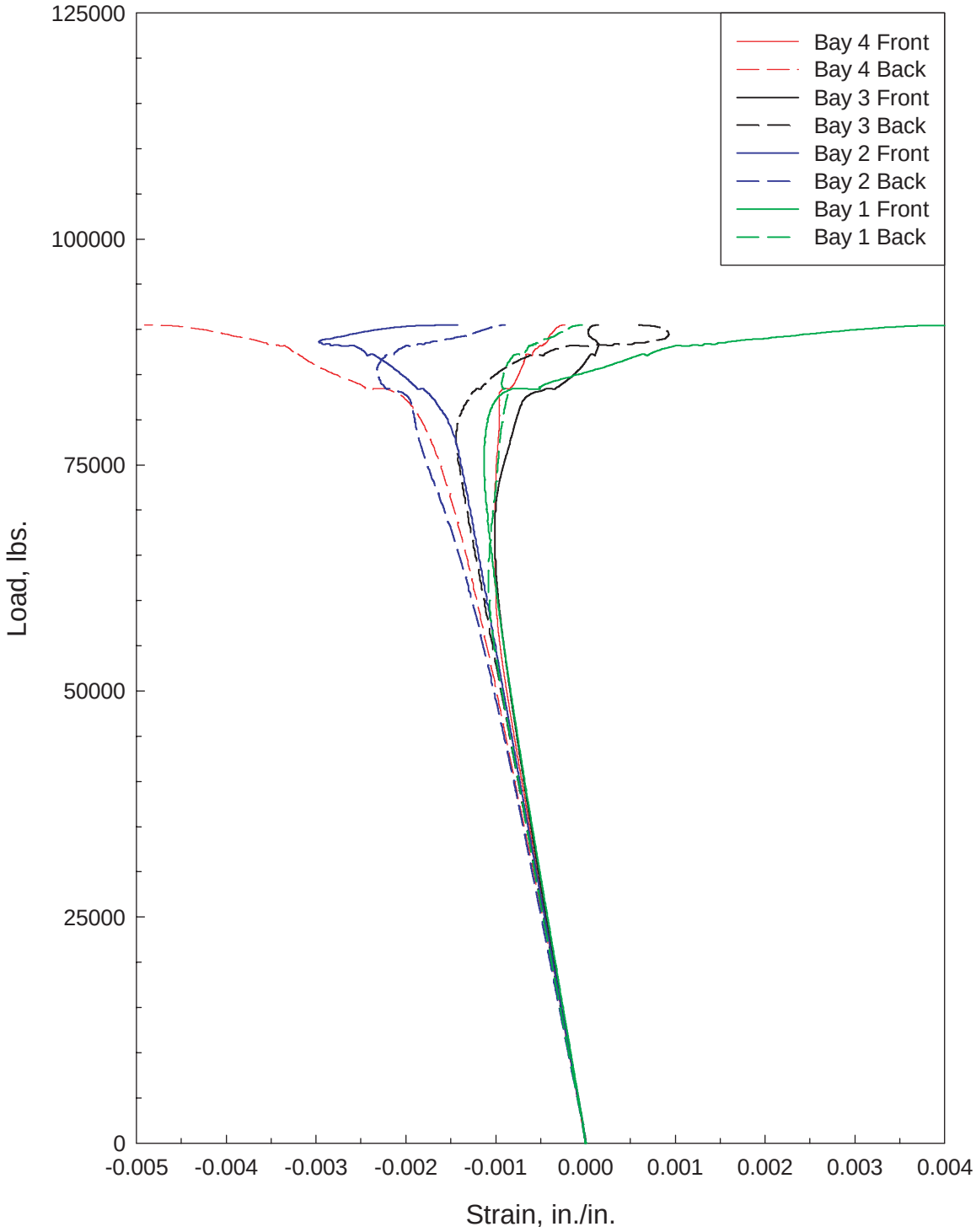

Figure 16. Strains at the centerline of the friction stir welded panel bays. Solid lines represent the bay skin strains on the front, or stiffener, side of the panel and dashed lines represent the bay skin strains on the back, or unstiffened, side of the panel.

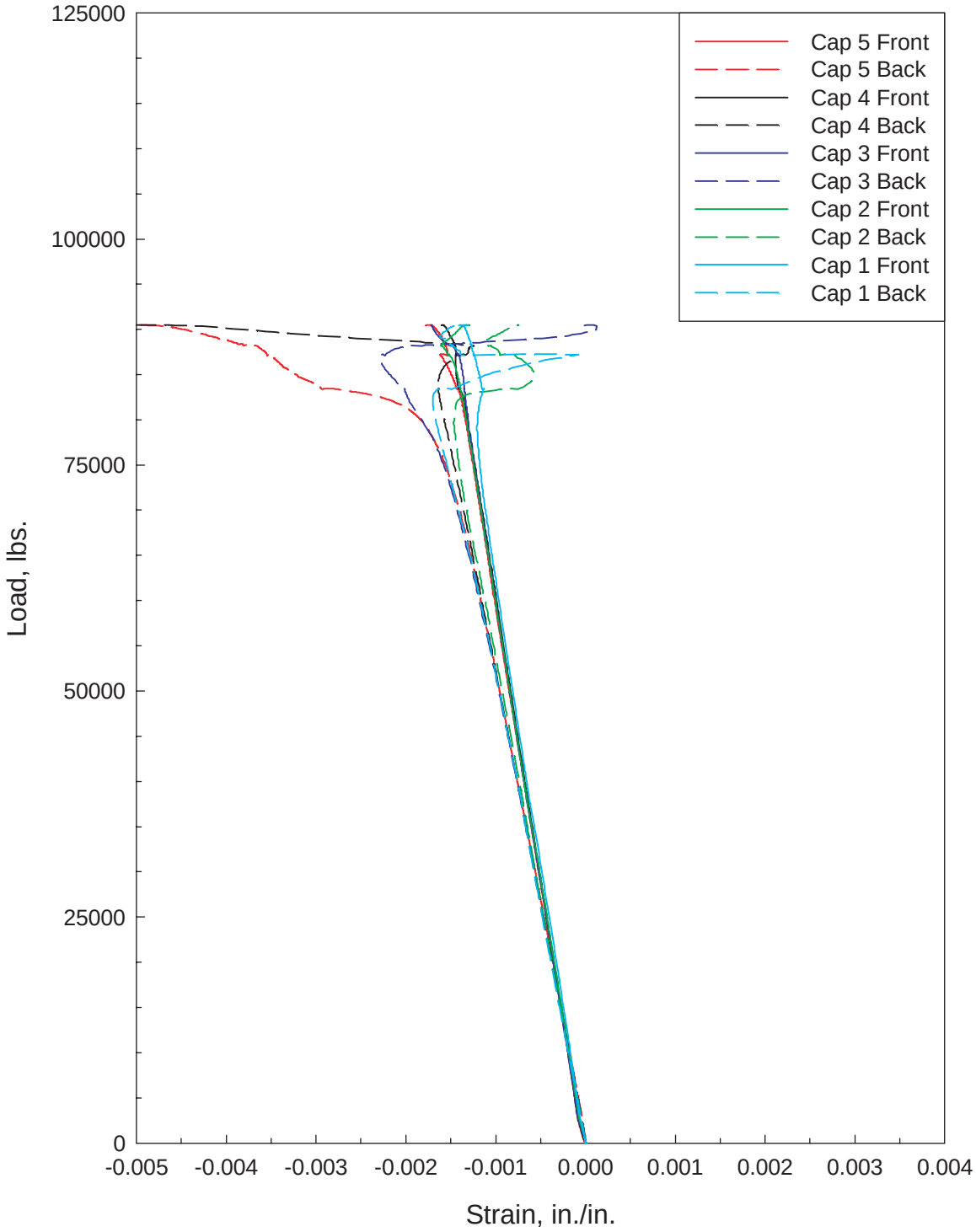

Figure 17. Strains at the centerline of the friction stir welded panel stiffeners. Solid lines represent the strains on the top of the stiffener caps and the dashed line represent the strains on the skin beneath the stiffeners on the back, or unstiffened, surface.

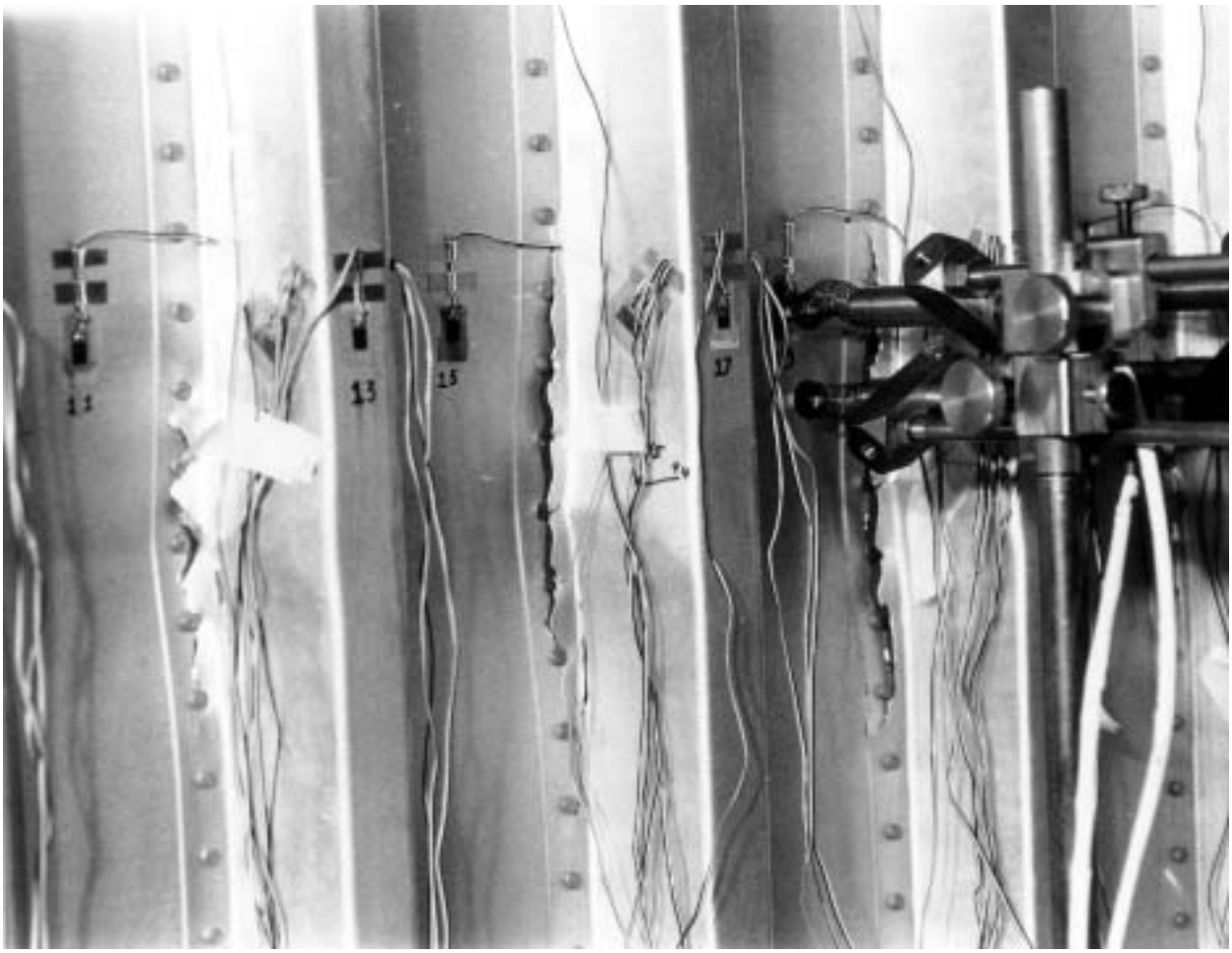

(a) Buckle at centerline of panel.

Figure 18. Buckled riveted panel.

(b) Stiffener at centerline of panel showing stiffener failure at rivets and cap.

Figure 18. Concluded.

(a) Buckle at centerline of panel.

Figure 19. Buckled friction stir welded panel.

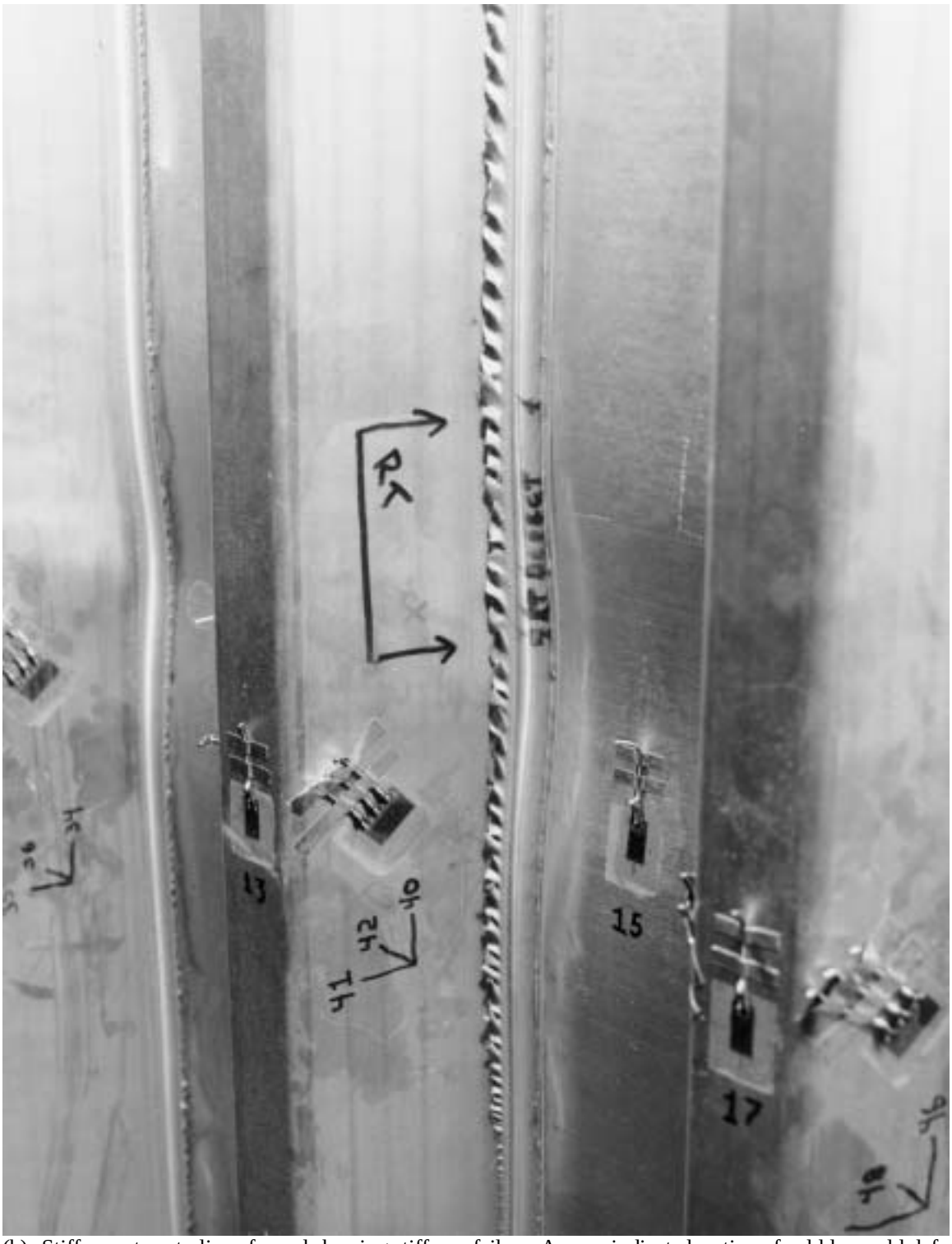

(b) Stiffener at centerline of panel showing stiffener failure. Arrows indicate location of cold lap weld defect.

Figure 19. Concluded.

REPORT DOCUMENTATION PAGE

Form Approved
OMB No. 0704-0188

1. REPORT DATE *(DD-MM-YYYY)*	2. REPORT TYPE	3. DATES COVERED *(From - To)*
08-2002	Technical Memorandum	

4. TITLE AND SUBTITLE

Compression Buckling Behavior of Large-Scale Friction Stir Welded and Riveted 2090-T83 Al-Li Alloy Skin-Stiffener Panels

5a. CONTRACT NUMBER

5b. GRANT NUMBER

5c. PROGRAM ELEMENT NUMBER

6. AUTHOR(S)

Eric K. Hoffman, Robert A. Hafley, John A. Wagner, Dawn C. Jegley, Robert W. Pecquet, Celia M. Blum, and William J. Arbegast

5d. PROJECT NUMBER

5e. TASK NUMBER

5f. WORK UNIT NUMBER

713-50-02-51

7. PERFORMING ORGANIZATION NAME(S) AND ADDRESS(ES)

NASA Langley Research Center
Hampton, VA 23681-2199

8. PERFORMING ORGANIZATION REPORT NUMBER

L-18195

9. SPONSORING/MONITORING AGENCY NAME(S) AND ADDRESS(ES)

National Aeronautics and Space Administration
Washington, DC 20546-0001

10. SPONSOR/MONITOR'S ACRONYM(S)

NASA

11. SPONSOR/MONITOR'S REPORT NUMBER(S)

NASA/TM-2002-211770

12. DISTRIBUTION/AVAILABILITY STATEMENT

Unclassified - Unlimited
Subject Category 39
Availability: NASA CASI (301) 621-0390 Distribution: Standard

13. SUPPLEMENTARY NOTES

Hoffman, Hafley, Wagner, and Jegley: Langley Research Center; Pecquet and Blum: Lockheed-Martin Space Systems; Arbegast: South Dakota School of Mines and Technology
An electronic version can be found at http://techreports.larc.nasa.gov/ltrs/ or http://techreports.larc.nasa.gov/cgi-bin/NTRS

14. ABSTRACT

To evaluate the potential of friction stir welding (FSW) as a replacement for traditional rivet fastening for launch vehicle dry bay construction, a large-scale friction stir welded 2090-T83 aluminum-lithium (Al-Li) alloy skin-stiffener panel was designed and fabricated by Lockheed-Martin Space Systems Company - Michoud Operations (LMSS) as part of NASA Space Act Agreement (SAA) 446. The friction stir welded panel and a conventional riveted panel were tested to failure in compression at the NASA Langley Research Center (LaRC). The present paper describes the compression test results, stress analysis, and associated failure behavior of these panels. The test results provide useful data to support future optimization of FSW processes and structural design configurations for launch vehicle dry bay structures.

15. SUBJECT TERMS

Al-Li alloy; 2090; friction stir welding; FSW; rivet; buckling; compression

16. SECURITY CLASSIFICATION OF:			17. LIMITATION OF ABSTRACT	18. NUMBER OF PAGES	19a. NAME OF RESPONSIBLE PERSON
a. REPORT	b. ABSTRACT	c. THIS PAGE			STI Help Desk (email: help@sti.nasa.gov)
					19b. TELEPHONE NUMBER *(Include area code)*
U	U	U	UU	41	(301) 621-0390